Research article

Title

Application of proteomic profiling based on 2D-DIGE for classification of compounds according to the mechanism of action.

Authors and Affiliations

Makoto Muroi[1], Sayaka Kazami[1, 2], Kazue Noda[1], Hisae Kondo[1], Hiroshi Takayama[1, 2], Makoto Kawatani[1], Takeo Usui[3], and Hiroyuki Osada[1, 2]

1) Chemical Library Validation Team, Chemical Biology Core Facility, Chemical Biology Department, RIKEN Advanced Science Institute, 2-1 Hirosawa, Wako-shi, Saitama 351-0198, Japan
2) Graduate School of Science and Engineering, Saitama University, 255 Shimo-Okubo, Saitama 338-8570, Japan
3) Graduate School of Life and Environmental Sciences, University of Tsukuba, Tsukuba, Ibaraki 305-8572, Japan

Contact: Hiroyuki Osada, PhD,
Chemical Biology Department, RIKEN Advanced Science Institute, 2-1 Hirosawa, Wako-shi, Saitama, 351-0198, Japan
Fax: +81-48-462-4669, E-mail: hisyo@riken.jp

Running Title

Proteomic profiling for classification of compounds

Additional Footnote

Abbreviations: HSP, heat shock protein; IC_{50}, 50% inhibitory concentration; Topo II, topoisomerase II

SUMMARY

The development of new anticancer agents derived from natural resources requires a rapid identification of their molecular mechanism of action. To make this step short we have initiated the proteomic profiling of HeLa cells treated with the anticancer drugs representing a wide spectrum of mechanisms of action, using 2D-DIGE. A unique proteome patterns were observed in HeLa cells treated with the HSP90 inhibitor, geldanamycin, and those were similar to the patterns induced by radicicol, another structurally different HSP90 inhibitor. On the other hand, etoposide and ICRF-193, the compounds claimed to be topoisomerase II inhibitors, showed different proteomic profiles, which reflect their different biological activities as revealed by cell cycle analysis. So far combined data from 19 compounds allowed their successful classification by cluster analysis according to the mechanism of action.

INTRODUCTION

Cell based assays are widely used in drug discovery because the assessment of molecular interaction occurs within the context of a living cellular environment (Baker, et al., 2007). Many bioactive compounds, inhibiting the growth of cancer cells, have been isolated using a cell-based screen (Kakeya, et al., 2002; Kawada, et al., 2009). In most instances, the molecular target for newly isolated compounds remained unknown. The identification of a plausible target is sometimes possible based on the results of cell-based assays, however, the exact target must be proven by enzymatic assays, analyses of binding proteins, or genetic methods employing a siRNA (Kazami, et al., 2006; Sato, et al., 2007; Teruya, et al., 2005). The confirmation of the molecular targets, however, is usually a difficult and time-consuming process.

The multidimensional phenotype profiling approaches have a capacity to generate a testable hypothesis related to the mechanism of action and eventual off-target effects of new compounds. The differential sensitivity of the panel of cancer cell lines to the compounds has been used to identify their molecular target(s). The most commonly used assay, NCI 60 antitumor screen, allowed to identify benzolactone enamide as an inhibitor of V-ATPase (Boyd, et al., 2001). The other panel consisting of 39 different cancer cell lines identified the compound encoded as ZSTK474 to be the inhibitor of phosphatidylinositol 3-kinase (Yaguchi, et al., 2006). Recent advances in the field of molecular biology provided a wide spectrum of methods suitable for target identification. The application of the connectivity map, developed by Golub and co-workers that uses gene expression signature for profiling (Lamb, et al., 2006), led to the identification of a class of HSP90 pathway modulators (gedunin and celastrol) (Hieronymus et al 2006). The cell morphology-based profiling (Abassi, et al., 2009; MacDonald, et al., 2006) and the activity-based proteomic profiling (Leung, et al., 2003) are also used for molecular target identification.

Compared with gene expression profiling which can simultaneously measure the expression of more than 20,000 genes, proteome analysis provides us only with the opportunity to trace at most 1,000 protein spots. However, any change of molecular weight and isoelectric point of proteins after posttranslational modification is often detectable as a mobility shift of protein spots in two-dimensional gel electrophoresis (2DE) analyses. Since biologically active compounds affect cellular processes and induce changes in both the expression levels and modification of proteins, proteome

profiling is an informative approach for investigating the effects of the compound. Indeed, several research groups have shown that biologically active compound alter the proteome (Cecconi, et al., 2007; Towbin, et al., 2003). Recent advances in two-dimensional difference gel electrophoresis (2D-DIGE) have allowed to measure the abundance of each protein spot between different gels with a high accuracy due to introduction of an internal standard (Van den Bergh and Arckens, 2004). With 2D-DIGE, the abundant proteomic expression data obtained from different treatments can be collected, and the expression patterns can be compared. In this study, we have used 2D-DIGE to perform a comprehensive proteome analysis of protein expression changes caused by the treatment of cancer cells with the anticancer drugs claimed to possess the "exact mechanisms of action".

It is well known that the anticancer drugs of known and similar mechanism of action such as doxorubicin and daunorubicin, both classified as anthracyclines, are clinically active against different types of cancers. Doxorubicin is mainly used in the treatment of solid tumors, while daunorubicin shows activity in hematologic malignancies. The other case is cisplatin and oxaliplatin, the former active against lung and ovarian cancers, and the latter active against colon cancer. Keeping in mind a subtle difference in clinical activity of the compounds of similar "exact mechanism of action", we have made an attempt to establish differential proteins profiles in cancer cells treated with anticancer agents representing several main mechanisms of action, including also several compounds possessing the same well-established mechanism of action. The proteomic profiling of mechanism of action may play essential role in the planning of individualized chemotherapy of cancer patients, once the correlation between drug sensitivity and the drug-induced proteomic profile is found.

Here, we report the procedure and results of the proteome analysis, using 2D-DIGE that revealed significant similarities in protein expression changes induced by the compounds belonging to the same class. Furthermore, we were also able to distinguish subtle differences among compounds attacking the same molecular target, however, in a different way.

RESULTS

Proteomic Patterns of Geldanamycin and Radicicol-Treated HeLa Cells are Similar

Geldanamycin (**1**) and radicicol (**2**) are well-known HSP90 inhibitors (Schulte, et al., 1998; Whitesell, et al., 1994). HSP90 is one of the targets for cancer therapeutics, and 17-AAG, a derivative of geldanamycin is under clinical trials (Nowakowski, et al, 2006). First, we have determined cell growth inhibitory effect of HSP90 inhibitors against HeLa cells using a WST-8 assay (Fig. 1A). The IC_{50} growth inhibitory concentration of geldanamycin against HeLa cells was approximately 0.05 μM in a 48-h treatment. HeLa cell growth was not affected at concentrations lower than 0.01 μM, while a complete growth inhibition was observed at concentrations greater than 0.1 μM. The IC_{50} of radicicol against HeLa cell growth was approximately 1 μM.

Next, we have investigated the relationship between proteomic changes after exposing HeLa cells to effective concentrations of the compounds, e. g., 0.005, 0.05, 0.5, 5, and 10 μM for geldanamycin and 10 μM for radicicol; the results are shown in Fig. 1B. In this analysis, 775 spots in 2DE gels were matched on all gel images and quantified by 2D-DIGE system software, resulting in 282 spots that were selected by ANOVA ($P < 0.01$) and Dunnett's test ($P < 0.01$) (see Table S1). Then, hierarchical cluster analysis was performed. The results were displayed in the form of a heat map and a tree diagram (Fig. 1B). In the heat map, the spots with increased expression are indicated in red, and the spots with decreased expression are indicated in green. As indicated in the tree diagram and the heat map, the patterns of protein expression were similar at geldanamycin concentrations greater than 0.5 μM.

To simplify the statistical evaluation of the 2D-DIGE experiments, the spots that were modified significantly between groups were typically selected using ANOVA test and a volume ratio filter of no less than 2-fold for 3 biological replicates per group (Karp and Lilley, 2005). Using these parameters, 17 spots were selected and a similar result for the cluster analysis was obtained (data not shown).

In HSP90 inhibitor-treated cells, HSP70 and HSP27 have been reported to be upregulated (Maloney, et al., 2007; McCollum, et al., 2006). To classify test compounds using proteomic profiling, the identity of each protein spot is not necessary, however, it is important to confirm whether proteomic change of geldanamycin-treated cell matches that in previously reported results. Peptide mass fingerprinting identified 20 spots out of the total number of spots that had been significantly affected by the treatment with

geldanamycin and other compounds (Table S2 and S3). The application of ANOVA test selected 15 out of 20 spots and the mean ratios between control and inhibitor-treated cells were tabulated (Table 1).

Spots 1114 and 1127, which were identified as heat shock 70 kDa protein 1 (HSP70, *HSPA1B*), were upregulated more than 7-fold when compared with control. At 0.05 μM geldanamycin, HSP70 upregulation was also detected, but the magnitude of increase was lower compared with higher concentrations. The expression level of spot 2382, identified as heat shock protein beta-1 (HSP27, *HSPB1*), also reached a plateau, as did HSP70. By Western blot, both HSP70 and HSP27 were upregulated to similar extent at concentrations greater than 0.05 μM (Fig. 1C).

The upregulation of mitochondrial heat shock proteins (*HSP9B*, *HSPD1*) and protein disulfide isomerase and downregulation of eukaryotic elongation factor 2 (*EEF2*), fascin (*FSCN1*), adenylyl cyclase-associated protein 1 (*CAP1*), and aldo-keto reductase family 1 member C2 (*AKR1C2*) were observed in geldanamycin-treated HeLa cells. It is very important to indicate that the concentration corresponding to the IC_{50} in the WST-8 assay is insufficient to induce any obvious changes in the proteomic analysis. It is more reasonable to use concentrations at which cell growth is nearly completely inhibited.

When the cells were exposed to 0.5 μM geldanamycin, the amount of HSP70 increased in time-dependent manner and reached a plateau after 18 h (Fig. 1 D and E). Since long incubation with test compounds may be associated with secondary effects, such as apoptosis, we purposely avoided long exposures. Instead, we performed a subsequent proteomic analysis of HeLa cells after 18 h exposure to test compound.

Radicicol (**2**) is another HSP90 inhibitor that structurally differs from geldanamycin (**1**). The expression patterns between radicicol- and geldanamycin-treated cells were compared by 2D-DIGE. Similar responses were observed between geldanamycin- and radicicol-treated cells (Fig. 1B and Table 2). HSP70 (nos. 1114 and 1127), HSP27 (nos. 2372 and 2382) and 78 kDa glucose-regulated protein (GRP78, *HSPA5*; nos. 972 and 983) increased during both treatments (Table 2). The spots representing eukaryotic elongation factor 2, fascin, and adenylyl cyclase-associated protein 1 were downregulated during both treatments. These results strongly suggest that compounds inhibiting the same molecular target generate similar proteomic profiles.

Proteomic Analysis of HeLa Cells Treated with Compounds of Known Mechanisms of Action

To compare the proteomic patterns in HeLa cells treated with the compounds whose targets are known, the well-characterized chemical entities were selected for proteomic analysis (Table 2). Based on experience with geldanamycin, the proteomic analysis of above mentioned compounds was performed at the concentrations higher than their respective IC_{50} values. Their growth inhibitory effects were determined by WST-8 assay and are presented as the IC_{50} values in Table 2. The concentrations used for the exposure of HeLa cells during proteomic profiling experiments were those inhibiting cell growth by 80% or more (Table 2).

As previously indicated, the proteomic analyses of HeLa cells were performed after 18 h exposure to a test compound. Since the master gel of geldanamycin-treated cells from the previous experiment (Fig. 2A) was used as the template, the numbering of the spots remained the same in all experiments. Three hundred eighteen spots in the 2DE-gel were matched on all gel images, and quantified by 2D-DIGE software; 298 of them were selected by ANOVA ($P < 0.01$) and Dunnett's test ($P < 0.01$) (see Table S4). The data were calculated and visualized by cluster analysis programs (Fig. 2B); the mean ratio of the identified spots and the results of statistical analysis are listed in Table 4.

As indicated in the tree diagram (Fig. 2B), the inhibitors of V-ATPase (bafilomycin A1 and concanamycin A), tubulin (nocodazole and vinblastine), and actin (cytochalasin D and jasplakinolide) were classified into separate clusters. The spots that changed significantly between groups were selected using ANOVA and a volume ratio filter of no less than 2-fold (Karp and Lilley, 2005), yielding 47 spots and leading to a similar result of cluster analysis (data not shown).

We also noticed that MG-132, a proteasome inhibitor, generated a similar pattern as the HSP90 inhibitors did. The amount of protein in the HSP70 spots (spots 1114 and 1127) also increased in MG-132-treated cells, as did those observed in geldanamycin- and radicicol-treated cells (Table 3). In contrast, the HSP27 showed an aberrant pattern. Although HSP90 inhibitors increased the amount in spots 2372 and 2382, which were identified as HSP27, the MG-132 treatment increased only the spot number 2372.

Other noteworthy changes were as follows: 1) the inhibitors of actin, cytochalasin D and jasplakinolide increased the amount of actin (spots 1758 and 1767); 2) tunicamycin increased the spot 983, identified as GRP78, 4.6-fold compared with control; 3)

ICRF-193 and antimicrotubular agents, such as nocodazole and vinblastine, decreased the amount of lamin (970 and 978) in consequence forming one cluster; and 4) the potent protein kinase inhibitor staurosporine downsized the spots 714 (*EEF2*), 970 (*LMNA*), 1227 (*HNRNPK*), 1429 (*CAP1*), and 1484 (*FSCN1*), while expanding the spots 983 (*HSPA5*), 998 (*HSPA9B*), 1295 (*HSPD1*), 1767 (*ACTG1*), and 2382 (*HSPB1*).

Iejimalides, 24-membered macrolides, were originally isolated from marine tunicate as potent antitumor compounds (Nozawa, et al., 2006). We recently found that iejimalides inhibited V-ATPase (Kazami, et al., 2006). We have analyzed HeLa cells treated with iejimalide A (**3**) or iejimalide B (**4**) at 30 nM by 2D-DIGE. We combined the proteome data from iejimalides-treated HeLa and compared with the proteomic profiles generated by the treatment of HeLa cells with 19 well-characterized compounds. Iejimalide A (**3**) and B (**4**) were clustered into the same tree as the other V-ATPase inhibitors (e.g., bafilomycin A1 (**5**) and concanamycin A (**6**)) (Fig. 2C). Recently, it was reported that iejimalides affect actin depolymerization (Fürstner, et al., 2007), however, iejimalide A and B did not match the cluster representing actin inhibitors. These results indicate that the primary target of iejimalides in HeLa cells is V-ATPase, at least at concentration used in our experimental setting.

Flow Cytometry of HeLa Cells Treated with ICRF-193 and Etoposide

The proteomic analysis of HeLa cells treated with the two structurally different inhibitors of topoisomerase II (topo II), ICRF-193 (**7**) and etoposide (**8**) revealed significant differences; both compounds were not able to form a single cluster (Fig. 2B). To confirm this finding, we measured the distribution of cellular DNA in HeLa cells by flow cytometry, after treating asynchronous HeLa cells with varying concentrations of ICRF-193 or etoposide for 48 h.

The basic amount of DNA in a haploid nucleus is given the value C. In the absence of inhibitors, we observed typical 2 peaks, corresponding to cell population with 2C and 4C DNA content. The treatment of HeLa cells with ICRF-193 resulted in decreasing the height of the 2C peaks at concentrations higher than 1 μM, while the 4C population increased (Fig. 3A). On the other hand, etoposide used at concentrations higher than 1 μM also increased the 4C peaks, but without any obvious accumulation of the peaks containing 8C DNA, contrasting the effect of ICRF-193 (Fig. 3B).

The kinetics of the shifts from the diploid to tetraploid DNA cellular contents was also studied in time-dependent fashion, using equimolar concentration of 10 μM for both test compounds. The ICRF-193 induced a gradual accumulation of 4C population up to 18 hour, then the generation of polyploidy (8C) in HeLa cells was observed (Fig. 3C) beyond that time point.

Etoposide was not able to induce polyploidy in HeLa cells, even during 72-h exposure (Fig. 3D). Despite the presence of common mechanism of action (topo II inhibition), the final biological effects are different, and two compounds were clustered into different cluster in our proteomic analysis.

DISCUSSION

In this study, we have performed a proteomic analysis of HeLa cancer cells treated with well-characterized anticancer agents using a 2D-DIGE system. The target proteins of these compounds are known at the cellular level and represent the targets for cancer therapeutics, such as the proteasome and microtubules. Each compound induced a characteristic proteomic pattern and hierarchical clustering exactly classified the compounds according to their respective targets, such as HSP90, tubulin and V-ATPase (Fig 2B).

Topo II inhibitors are still good candidates for molecular targeted drugs in cancer therapy. Topo II as a single target can be inhibited by two distinct mechanisms. One is exercised by a catalytic site inhibition, resulting in the formation of a non-cleavable complex and is characteristic for ICRF-193, a topo II inhibitor (**7**) (Roca, et al., 1994; Tanabe, et al., 1991). The other mechanism involves the stabilization of DNA cleavable complex, which further leads to double-strand DNA breaks and damage; etoposide (**8**), a topo II poison, plays essential role in this mechanism (Liu, 1989). As reported by Ishida et al., etoposide blocked the progression of cells to M phase, while ICRF-193 only delayed the transition from S to M phase and induced polyploidization in HeLa cells (Ishida, et al., 1994). Thus, both compounds are topo II inhibitors but act through disparate mechanisms (Andoh and Ishida, 1998). Their proteomic phenotypes differed and did not fall into the same cluster. Moreover, their cellular phenotypes, as determined by the analysis of cellular DNA distribution (Fig. 3) differed as well. One may conclude that such compounds can be classified into different clusters from proteomic point of view, despite exercising their biological activity through the same molecular target, or their exact mechanism of action may be revised. An inability to share a common cluster might be caused by an excessive off-target effect. To clarify that matter it seems important to know which mechanism determines anticancer activity against particular type of cancer or contributes mainly to toxicity. Gathering more data will be of a great importance in the evaluation of undesired effects as well.

So far, our proteomic profiling of mechanism of action of anticancer agents appeared to be helpful in the identification of the mode of action of iejimalides, a newly isolated natural products, as being inhibitors of V-ATPase (Fig. 2C). The comparison of the proteomes of the cells treated with a newly isolated compound versus well-characterized

compounds can lead to the testable hypothesis on general mechanisms of action as in the case of other profiling approaches such as the genetic one.

Despite of recent enthusiasm, one may anticipate certain limitations of our proteome profiling system. To name a few, the following factors may become the obstacle in the system. 1) The suspected target for test compound is not expressed or is not functional (mutation, SNP) in HeLa cells. 2) The suspected target was not validated yet by known standards. 3) The changes induced in proteomic profile by a test compound are not sufficiently distinct due to the appearance of limited number of spots in 2D gels. 4) The presence of several molecular targets may complicate the analysis; therefore, an interpretation of data will have to be made with great caution.

Our proteomic analysis matched methyl-gerfelin with two V-ATPase inhibitors, however, its biological effects in cell system (upregulation of pH, Figure S1) were not confirmed. The newly developed by us technology of a small molecule affinity matrix, revealed a strong interaction with glyoxalase I, supposedly a direct target molecule (Kawatani et al., 2008). The lack of standards for glyoxalase I inhibitors in proteomic analysis led to the clustering with the V-ATPase inhibitors. Therefore, the expansion of the system by variety of compounds with increased precision and accuracy of the system in classifying compounds into groups will lead to the well-established mechanism of action. The compounds not matching any known mechanisms may be considered as the probes for searching not yet identified molecular targets.

The case of jasplakinolide and cytochalasin D may well illustrate some of the obstacles, both compounds affect actin by inhibiting its depolymerization (Bubb, et al., 1994) and polymerization (Cooper, 1987), respectively. Although their effects on actin are opposed, both compounds increased the levels of actin and were included into the same cluster in this experiment. However, we noted the presence of several unidentified spots that did not correlate to these two compounds. Further investigation should clarify the differences between polymerizing and depolymerizing effects of these two inhibitors with the application of proteomic analysis.

The 2DE-based proteomic analysis is generally a time-consuming process during the initial stage of system development, since the identification of almost all protein spots is essential. Once this stage is completed and a database is created, one can analyze the proteomic profiles of many chemical entities by comparing them with those contained in the database, without necessity of additional protein spots identification. This is a huge

advantage of this technique. Nevertheless, in the case of dramatic change in the expression levels among not yet identified spots, the characterization of those spots will be very informative in target identification, or at least these compound-specific spots may serve as an important marker of biological activity. The agents inducing microtubules depolymerization may serve as an illustration of where a compound does not directly cause the modification of a protein spot, and is rather an artifact related to its primary mechanism of action. More specifically, the antimicrotubular agents cause cell cycle arrest in M-phase, preventing cell division due to the lack mitotic spindle formation and the nuclear envelope remains intact. Under normal condition the envelope is broken down and its component, lamin, is released (Parnaik, 2008). The release of lamin is decreased after the exposure of the cells to antimicrotubular agents (Table 3) and may serve as a marker of compound's effectiveness, albeit, not being a target.

The treatment of HeLa cells with MG-132 increased the expression of HSP70, thus confirming already reported phenomenon (Kawazoe, et al., 1998) and the cluster analysis tree positioned this compound close to the group of HSP90 inhibitors. However, slight differences were observed, namely, HSP90 inhibitors increased both spots of HSP27 (nos. 2372 and 2382), while the MG-132 increased only spot number 2372. Because HSP27 has been reported to enhance proteasome-dependent protein degradation (Parcellier, et al., 2006; Parcellier, et al., 2003), this result may suggest the presence of at least two forms of HSP27, one of which is probably involved in proteasome-dependent protein degradation. Based on these results, we propose that the expression levels of HSP27 spots may determine the classification of compounds either to HSP90 inhibitor or to proteasome inhibitor class of compounds. Particularly, the expression ratio of HSP70 and HSP27 spots will play a role of differentiating marker for either class.

So far, we have examined only 19 compounds, reaching an ability to classify the compounds according to their mechanism of action. The expansion of the proteomic profiling by the other types of compounds with different mode of action will make the system fully operating for the prediction of biological activity of newly discovered natural products or synthetic compounds. Already, we were able to classify a newly synthesized derivative of natural product with unknown mechanism of action as an inhibitor of topoisomerase II (data not shown). For that purpose, the extensive process of system validation using the chemical library of NPDepo (Tomiki, et al., 2006) is under way. Since the assay is primary based upon the only one cancer cell line, it is reasonable

to include the other cell lines, especially when the obvious differences in drug responses among cell line are observed. As the natural consequence of the recent promising results, there is the need to include protein interaction map that should enforce the discovery of new target molecules. One may easily indicate a protein spot which may become a marker, however, one should explore the path from the marker up to the protein responsible for that change; then the protein may be claimed to be a target, or in other words, the object of a primary attack by an active substance.

In summary, the proteomic profiling based on the 2D-DIGE is an important supplement to other multidimensional phenotypic profilings and its capacity may be extended by the introduction of the different pathological phenotypes represented by cancer cells, leading, e.g., to identification of specific biomolecules as well.

SIGNIFICANCE

New natural compounds, possessing important biological activity, had been subjected to extensive and time-consuming processes to clarify main mechanism of action. In order to reduce the time for target identification, we set up the faster method based on a 2D-PAGE characteristic proteomic patterns of HeLa cells treated with various compounds. The compounds such as geldanamycin and radicicol, representing diverse structures but sharing common target, were classified in the same tree by cluster analysis. The iejimadiles A and B, were reported to affect depolymerization of actin, however, were not clustered together with actin inhibitors, instead were clustered into a group of V-ATPase inhibitors, as have been confirmed by the direct inhibitory effect of iejimalides A and B on V-ATPase (Biosci. Biotechnol. Biochem. *70*, 1364-1370). Furthermore, when different type of topo II inhibitors, etoposide and ICRF-193, which are known as a topo II poison and a catalytic inhibitor, respectively, were analyzed by the system, the compounds were clustered into different trees. This indicates a power of the system that discriminates compounds by mechanism of action. The expansion of the database of proteomic profiling by a 2D-PAGE will aid the characterization of numerous natural compounds in many aspects, such as mechanism of action, off-target effects, biomarking, and yet unknown target(s) identification.

EXPERIMENTAL PROCEDURES

Materials

Iejimalide A and B were obtained from Dr. Jun'ichi Kobayashi of Hokkaido University. Actinomycin D, brefeldin A, concanamycin A, cycloheximide, cytochalasin D, geldanamycin, radicicol, staurosporine and etoposide were provided by the NPDepo (RIKEN Natural Products Depository, http://www.npd.riken.jp/npd/). Bafilomycin A1, daunomycin, and tunicamycin were purchased from Wako Pure Chemical Industries (Osaka, Japan). Okadaic acid and nocodazole were purchased from Sigma (St. Louis, MO). Jasplakinolide, LY294002, MG-132, and vinblastine were from Calbiochem (La Jolla, CA). ICRF-193 was from Funakoshi Co. Ltd. (Tokyo, Japan).

All compounds were dissolved in dimethylsulfoxide (DMSO) and stocked at -20°C. Monoclonal anti-HSP70 (clone C92F3A-5) and monoclonal anti-HSP27 (clone G3.1) were purchased from Stressgen Biotechnologies Corporation (British Columbia, Canada). Monoclonal anti-α-tubulin (clone DM1A) was purchased from Sigma (St. Louis, MO). The reagents for Western blotting were purchased from Thermo Scientific (Rockfort, IL). All reagents were reagent-grade.

Cell Culture

HeLa cells were cultured in Dulbecco's Modified Eagle's Medium (D-MEM, Sigma, St. Louis, MO), supplemented with 10% fetal bovine serum, at 37°C in a humidified CO_2 incubator (5% CO_2-95% air).

Cell Growth Assay

HeLa cells were seeded at 2×10^3 cells per well in a 96-well culture plate and incubated overnight, test compounds were added to the medium at various concentrations. After 48 h, cell number was determined using Cell Count Reagent SF (Nakalai Tesuque, Kyoto, Japan) according to the manufacturer's protocol. Briefly, 10 μL of WST-8 solution (mixture of WST-8 and 1-methoxy-5-methylphenazinium methylsulfate) was added to the wells and incubated for 2 h, and cell number was assessed by measuring the absorbance at 450 nm on a microplate reader (BIO-RAD, Hercules, CA)

Preparation of Cell Lysates for Proteomic Analysis

HeLa cells (3 x 10^5 cells) were seeded on a culture dish (35-mm diameter) containing 3 mL of medium and incubated overnight. Each assay was done in triplicates. The cells were exposed for 18h to the designated concentrations of test compounds. Cells were washed thrice with ice-cold phosphate-buffered saline (PBS), removed by a rubber policeman and collected by centrifugation at 4000 rpm for 3 min at 4°C in a microcentrifuge (KUBOTA 3700, Kubota, Tokyo, Japan).

After being washed once with PBS, cells were suspended in sample buffer (7 M urea, 2 M thiourea, 4% CHAPS, 30 mM Tris, buffered to pH 8.5) for 2D-DIGE and disrupted with a TOMY UR-20P sonicator (TOMY Co. Ltd., Tokyo, Japan). Cell lysates were treated with 1.25 U/μL benzonase (Merk, Darmstadt, Germany) for 60 min on ice and centrifuged at 12,000 rpm for 3 min at 4°C. Supernatants were stocked at -80°C until use.

Labeling of Cell Lysates and 2DE

Protein concentration was determined by Bradford procedure using the Protein Assay kit (BIO-RAD, Hercules, CA). Fifty micrograms of protein was labeled with 200 pmol of CyDye DIGE Fluor minimal dyes (GE Healthcare, Buckinghamshire, UK) according to the manufacturer's instructions (Cy3 and Cy5 for samples and Cy2 for internal control, consisting of equal parts of all samples in an experiment).

Samples were applied by rehydration onto immobilized pH gradient strips (24 cm, pH 3–10, nonlinear gradient, GE Healthcare) and subjected to isoelectrofocusing in an IPGphor IEF system (GE Healthcare). Strips were incubated in equilibration buffer (6 M urea, 30 % glycerol, 2% SDS, 50 mM Tris-HCl pH 8.8) containing 1% DTT for 15 min and then incubated in the same buffer containing 2.5% iodoacetamide for 15 min. Strips were transferred to the tops of 10% polyacrylamide gels and electrophoresed overnight in a DALT-twelve™ apparatus (GE Healthcare).

After electrophoresis, gels were scanned using a Typhoon™ 9400 imager at 100 dpi resolution (GE Healthcare). Gel analysis was performed using DeCyder BVA 6.5 (GE Healthcare), a 2DE analysis software package, following the manufacturer's recommendations. The estimated number of spots for each codetection was set to 3000.

Experimental Design and Data Processing for 2DE Profiling

To perform visual 2DE protein profiling of compound-treated HeLa cells, experiments were divided into subsets. We used the spot number of the master gel as the common master number for all of the experiments. The gel that contained the most spots in the first experiment (analysis of HeLa cells treated with various concentrations of geldanamycin) was chosen as the master gel.

In a representative subset of experiments, we used 3 compounds and DMSO. HeLa cells were treated with these solutions, and proteomic analysis was performed. All samples of compound- and DMSO-treated cells were prepared in triplicate. Equal parts of all samples in a subset of experiments were labeled with Cy2 CyDye Fluor as an internal standard.

To match the common master numbers between subsets of experiments, image files were imported into the project file, including the master gel, and spot maps of the images were matched to the master gel image using the BVA modules of DeCyder 6.5. More than 650 spots were usually matched in all the analyzed gels of a subset. The volume of each spot was obtained as a ratio of the Cy3- or Cy5-labeled sample compared with the corresponding Cy2 signal of the internal standard. Then, the volume of each spot was normalized using the average of the corresponding control value from the DMSO-treated HeLa cells.

Normalized volume data in subsets of experiments were combined, and only spots that did not lack data in any of the gels were selected. Subsequently, the spots that showed significant changes after compound-treatment were selected by ANOVA ($P < 0.01$) and Dunnett's test for post hoc analysis. For cluster analysis, the normalized volumes were calculated using the means of uncentered correlation with centroid linkage using Cluster 3.0 (Hoon, et al., 2004) and visualized using Java TreeView (Saldanha, 2004).

Statistical calculations, such as nonrepeated measures ANOVA and Dunnett's test for post hoc analysis (Sheskin, 2000), were performed using Microsoft Excel with a statistical macro (ystat2006, Igaku Tosho Shuppan, Tokyo, Japan) and R version 2.9.2 (http://cran.r-project.org/).

Western Blotting

Cell lysates were resolved by 10% SDS-PAGE and transferred to PVDF membranes. Membranes were blocked with 5% nonfat dried milk in TBS-T buffer (10 mM Tris-HCl, pH 8.0, 150 mM NaCl, and 0.05 % Tween 20), followed by incubation

with primary antibody (1:1000 dilution) in TBS-T. The detection was performed using horseradish peroxidase-labeled secondary antibodies (1:1000 dilution) and enhanced chemiluminescence detection reagent. The expression of tubulin was also measured and used as an internal control.

Flow Cytometry

Cells were treated with 0.25% trypsin for 5 min to remove them from the dish, washed with PBS, fixed in cold PBS containing 70% (v/v) ethanol, and stored at -20°C overnight. Then, the cells were washed with PBS and incubated with a DNA-staining solution containing 50 μg/ml propidium iodide (Sigma Chemical Co., St. Louis, MO) and 2 μg/ml RNase A at 4°C for 30 min. Total fluorescence intensities were determined by quantitative flow cytometry with Cytomics FC500 (Beckman Coulter, Miami, FL).

FIGURE LEGENDS

Figure 1. Dose- and Time-Dependent Effects of Geldanamycin and Radicicol on HeLa Cells

(A) Geldanamycin or radicicol was added at the indicated concentrations and incubated for 48 h. Cell number was measured by WST-8 assay, as described in Materials and Methods. Bars, SD (n = 3). (B) HeLa cells treated with a compound at the indicated concentrations or with DMSO for 18 h were analyzed by 2D-DIGE. Hierarchical clustering was performed. Red, upregulated; green, downregulated. The spots identified by peptide mass fingerprinting (PMF) (Table S2) are indicated by an arrow, and the master number and gene name are shown. (C) Cell lysates incubated for 18 h with designated concentrations of geldanamycin or radicicol were analyzed by Western blot following SDS-PAGE using anti-HSP70, anti-HSP27, or anti-tubulin. (D) HeLa cells were incubated in the presence of 0.5 μM geldanamycin for the indicated times and analyzed by 2-D DIGE. Using the data of 91 spots selected as described in Materials and Methods, hierarchical clustering was performed. The spots designated by the arrow are the spots (no. 1114, no. 1127) identified as HSP70 by PMF. (E) Mean ratios of spots 114 and 1127, determined in D, were plotted. Bars, SD (n = 3).

Figure 2. Clustering of Well-Characterized Compounds and Iejimalides by Proteomic Analysis of HeLa Cells

(A) HeLa cells treated with compounds listed in Table 2 for 18 h were analyzed by 2-D DIGE. The position of each spot is designated by a red circle, and the master number of the spot is marked. (B) Hierarchical clustering was performed. The identified spots (Table 3) are designated by arrows. (C) HeLa cells were treated with 30 nM of iejimalide A and B. The quantitive data was combined with the data of 19 well-characterized compounds and hierarchical clustering was performed.

Figure 3. Differential Phenotypes of HeLa Cells Treated with ICRF-193 and etoposide by Flow Cytometry.

The distribution of cellular DNA content of asynchronous HeLa cells treated with ICRF-193 or etoposide was determined by flow cytometry. HeLa cells were treated with the indicated concentrations of ICRF-193 (A) or etoposide (B) for 48 h. In a time course

experiment, HeLa cells were treated with 10 μM of ICRF-193 (C) or etoposide (D) for the indicated times.

ACKNOWLEDGMENTS

We would like to thank Dr. Jun'ichi Kobayashi in Hokkaido University for kindly providing Iejimalide A and B. We would like to thank Dr. Koji Kadota (University of Tokyo, Japan) for comments on the statistical calculations. We are grateful for the support of the Biomolecular Characterization Team in the RIKEN Advanced Technology Support Division for the MS analysis. We thank Dr. K. Wierzba, Dr. L. Zolt, Mr. E. Ong, and Mr. M. Khan for critical review of the manuscript. This study was supported in part by the Chemical Biology Project of RIKEN and grants from the Ministry of Education, Culture, Sports, Science, and Technology of Japan.

REFERENCES

Abassi, Y.A., Xi, B., Zhang, W., Ye, P., Kirstein, S.L., Gaylord, M.R., Feinstein, S.C., Wang, X., and Xu, X. (2009). Kinetic cell-based morphological screening: prediction of mechanism of compound action and off-target effects. Chem. Biol. *16*, 712-723.

Andoh, T., and Ishida, R. (1998). Catalytic inhibitors of DNA topoisomerase II. Biochim. Biophys. Acta. *1400*, 155-171.

Aubel-Sadron, G., and Londos-Gagliardi, D. (1984). Daunorubicin and doxorubicin, anthracycline antibiotics, a physicochemical and biological review. Biochimie *66*, 333-352.

Baker, D.D., Chu, M., Oza, U., and Rajgarhia, V. (2007). The value of natural products to future pharmaceutical discovery. Nat. Prod. Rep. *24*, 1225-1244.

Bialojan, C., and Takai, A. (1988). Inhibitory effect of a marine-sponge toxin, okadaic acid, on protein phosphatases. Specificity and kinetics. Biochem. J. *256*, 283-290.

Bowman, E.J., Sievers, A., and Altendorf, K. (1988). Bafilomycins: a class of inhibitors of membrane ATPase from microorganisms, animal cells and plant cells. Proc. Natl. Acad. Sci. U. S. A. *85*, 7972-7976.

Boyd, M.R., Farina, C., Belfiore, P., Gagliardi, S., Kim, J.W., Hayakawa, Y., Beutler, J.A., McKee, T.C., Bowman, B.J., and Bowman, E.J. (2001). Discovery of a novel antitumor benzolactone enamide class that selectively inhibits mammalian vacuolar-type (H^+)-atpases. J. Pharmacol. Exp. Ther. *297*, 114-120.

Bubb, M.R., Senderowicz, A.M., Sausville, E.A., Duncan, K.L., and Korn, E.D. (1994). Jasplakinolide, a cytotoxic natural product, induces actin polymerization and competitively inhibits the binding of phalloidin to F-actin. J. Biol. Chem. *269*, 14869-14871.

Cecconi, D., Donadelli, M., Rinalducci, S., Zolla, L., Scupoli, M.T., Scarpa, A., Palmieri, M., and Righetti, P.G. (2007). Proteomic analysis of pancreatic endocrine tumor cell lines treated with the histone deacetylase inhibitor trichostatin A. Proteomics *7*, 1644-1653.

Cooper, J.A. (1987). Effects of cytochalasin and phalloidin on actin. J. Cell Biol. *105*, 1473-1478.

Fürstner, A., Nevado, C., Waser, M., Tremblay, M., Chevrier, C., Teply, F., Aissa, C., Moulin, E., and Muller, O. (2007). Total synthesis of iejimalide A-D and assessment of the remarkable actin-depolymerizing capacity of these polyene macrolides. J. Am. Chem. Soc. *129*, 9150-9161.

Hieronymus, H., Lamb, J., Ross, K.N., Peng, X.P., Clement, C., Rodina, A., Nieto, M., Du, J., Stegmaier, K., Raj, S.M., et al. (2006). Gene expression signature-based chemical genomic prediction identifies a novel class of HSP90 pathway modulators. Cancer Cell *10*, 321-330.

Hoon, M.J.L.d., Imoto, S., Nolan, J., and Miyano, S. (2004). Open source clustering software. Bioinformatics *20*, 1453-1454.

Huss, M., Ingenhorst, G., König, S., Gassel, M., Dröse, S., Zeeck, A., Altendorf, K., and Wieczorek, H. (2002). Concanamycin A, the specific inhibitor of V-ATPases, binds to the V(o) subunit c. J. Biol. Chem. *277*, 40544-40548.

Ishida, R., Sato, M., Narita, T., Utsumi, K.R., Nishimoto, T., Morita, T., Nagata, H., and Andoh, T. (1994). Inhibition of DNA topoisomerase II by ICRF-193 induces polyploidization by uncoupling chromosome dynamics from other cell cycle events. J. Cell Biol. *126*, 1341-1351.

Kakeya, H., Onose, R., Koshino, H., Yoshida, A., Kobayashi, K., Kageyama, S., and Osada, H. (2002). Epoxyquinol A, a highly functionalized pentaketide dimer with antiangiogenic activity isolated from fungal metabolites. J. Am. Chem. Soc. *124*, 3496-3497.

Karp, N.A., and Lilley, K.S. (2005). Maximising sensitivity for detecting changes in protein expression: experimental design using minimal CyDyes. Proteomics *5*, 3105-3115.

Kawada, M., Momose, I., Someno, T., Tsujiuchi, G., and Ikeda, D. (2009). New atpenins, NBRI23477 A and B, inhibit the growth of human prostate cancer cells. J Antibiot (Tokyo) *62*, 243-246.

Kawatani, M., Okumura, H., Honda, K., Kanoh, N., Muroi, M., Dohmae, N., Takami, M., Kitagawa, M., Futamura, Y., Imoto, M., and Osada, H. (2008). The identification of an osteoclastogenesis inhibitor through the inhibition of glyoxalase I. Proc. Natl. Acad. Sci. USA *105*, 11691-11696

Kawazoe, Y., Nakai, A., Tanabe, M., and Nagata, K. (1998). Proteasome inhibition leads to the activation of all members of the heat-shock-factor family. Eur. J. Biochem. *255*, 356-362.

Kazami, S., Muroi, M., Kawatani, M., Kubota, T., Usui, T., Kobayashi, J., and Osada, H. (2006). Iejimalides show anti-osteoclast activity via V-ATPase inhibition. Biosci. Biotechnol. Biochem. *70*, 1356-1370.

Klausner, R.D., Donaldson, J.G., and Lippincott-Schwartz, J. (1992). Brefeldin A: insights into the control of membrane traffic and organelle structure. J. Cell Biol. *116*, 1071-1080.

Lamb, J., Crawford, E.D., Peck, D., Modell, J.W., Blat, I.C., Wrobel, M.J., Lerner, J., Brunet, J.P., Subramanian, A., Ross, K.N., et al. (2006). The Connectivity Map: using gene-expression signatures to connect small molecules, genes, and disease. Science *313*, 1929-1935.

Lee, D.H., and Goldberg, A.L. (1998). Proteasome inhibitors: valuable new tools for cell biologists. Trends Cell Biol. *8*, 397-340.

Leung, D., Hardouin, C., Boger, D.L., and Cravatt, B.F. (2003). Discovering potent and selective reversible inhibitors of enzymes in complex proteomes. Nat. Biotech. *21*, 687 - 691.

Lin, C.M., and Hamel, E. (1981). Effects of inhibitors of tubulin polymerization on GTP hydrolysis. J. Biol.Chem. *256*, 9242-9245.

Liu, L.F. (1989). DNA topoisomerase poisons as antitumor drugs. Annu. Rev. Biochem. *58*, 351-375.

MacDonald, M.L., Lamerdin, J., Owens, S., Keon, B.H., Bilter, G.K., Shang, Z., Huang, Z., Yu, H., Dias, J., Minami, T., et al. (2006). Identifying off-target effects and hidden phenotypes of drugs in human cells. Nat. Chem. Biol. *2*, 329-337.

Maloney, A., Clarke, P.A., Naaby-Hansen, S., Stein, R., Koopman, J.O., Akpan, A., Yang, A., Zvelebil, M., Cramer, R., Stimson, L., et al. (2007). Gene and protein expression profiling of human ovarian cancer cells treated with the heat shock protein 90 inhibitor 17-allylamino-17-demethoxygeldanamycin. Cancer Res. *67*, 3239-3253.

McCollum, A.K., Teneyck, C.J., Sauer, B.M., Toft, D.O., and Erlichman, C. (2006). Up-regulation of heat shock protein 27 induces resistance to 17-allylamino-demethoxygeldanamycin through a glutathione-mediated mechanism. Cancer Res. *66*, 10967-10975.

Nozawa, K., Tsuda, M., Ishiyama, H., Sasaki, T., Tsuruo, T., and Kobayashi, J. (2006). Absolute stereochemistry and antitumor activity of iejimalides. Bioorg. Med. Chem. *14*, 1063-1067.

Nowakowski, G.S., McCollum, A.K., Ames, M.M., Mandrekar, S.J., Reid, J.M., Adjei, A.A., Toft, D.O., Safgren, S.L., and Erlichman, C. (2006). A phase I trial of twice-weekly 17-allylamino-demethoxy-geldanamycin in patients with advanced cancer. Clin. Cancer Res. 12, 6087-6093.

Obrig, T.G., Culp, W.J., McKeehan, W.L., and Hardesty, B. (1971). The mechanism by which cycloheximide and related glutarimide antibiotics inhibit peptide synthesis on reticulocyte ribosomes. J. Biol. Chem. *246*, 174-181.

Parcellier, A., Brunet, M., Schmitt, E., Col, E., Didelot, C., Hammann, A., Nakayama, K., Nakayama, K.I., Khochbin, S., Solary, E., and Garrido, C. (2006). HSP27 favors ubiquitination and proteasomal degradation of p27Kip1 and helps S-phase re-entry in stressed cells. FASEB J. *20*, 1179-1181.

Parcellier, A., Schmitt, E., Gurbuxani, S., Seigneurin-Berny, D., Pance, A., Chantôme, A., Plenchette, S., Khochbin, S., Solary, E., and Garrido, C. (2003). HSP27 is a ubiquitin-binding protein involved in I-kappaBalpha proteasomal degradation. Mol. Cell. Biol. *23*, 5790-5802.

Parnaik, V.K. (2008). Role of nuclear lamins in nuclear organization, cellular signaling, and inherited diseases. Int. Rev. Cell Mol. Biol. *266*.

Rai, S.S., and Wolff, J. (1998). Localization of critical histidyl residues required for vinblastine-induced tubulin polymerization and for microtubule assembly. J. Biol. Chem. *273*, 31131-31137.

Roca, J., Ishida, R., Berger, J.M., Andoh, T., and C., W.J. (1994). Antitumor bisdioxopiperazines inhibit yeast DNA topoisomerase II by trapping the enzyme in the form of a closed protein clamp. Proc. Natl. Acad. Sci. U. S. A. *91*, 1781-1785.

Rüegg, U.T., and Burgess, G.M. (1989). Staurosporine, K-252 and UCN-01: potent but nonspecific inhibitors of protein kinases. Trends Pharmacol. Sci. *10*, 218-220.

Saldanha, A.J. (2004). Java Treeview—extensible visualization of microarray data. Bioinformatics *20*, 3246-3248.

Sato, S., Kwon, Y., Kamisuki, S., Srivastava, N., Mao, Q., Kawazoe, Y., and Uesugi, M. (2007). Polyproline-rod approach to isolating protein targets of bioactive small molecules: isolation of a new target of indomethacin. J. Am. Chem. Soc. *129*, 873-880.

Schulte, T.W., Akinaga, S., Soga, S., Sullivan, W., Stensgard, B., Toft, D., and Neckers, L.M. (1998). Antibiotic radicicol binds to the N-terminal domain of Hsp90 and shares important biologic activities with geldanamycin. Cell Stress Chaperones *3*, 100-108.

Sheskin, D.J. (2000). Handbook of parametric and non parametric statistical procedures, Second Edition (Boca Raton: CHAPMAN & HALL/CRC).

Sobell, H.M. (1985). Actinomycin and DNA transcription. Proc. Natl. Acad. Sci. U. S. A. *82*, 5328-5331.

Takatsuki, A., Arima, K., and Tamura, G. (1971). Tunicamycin, a new antibiotic. I. Isolation and characterization of tunicamycin. J. Antibiot. *24*, 215-223.

Tanabe, K., Ikegami, Y., Ishida, R., and Andoh, T. (1991). Inhibition of topoisomerase II by antitumor agents bis(2,6-dioxopiperazine) derivatives. Cancer Res. *51*, 4903-4908.

Teruya, T., Simizu, S., Kanoh, N., and Osada, H. (2005). Phoslactomycin targets cysteine-269 of the protein phosphatase 2A catalytic subunit in cells. FEBS Lett *579*, 2463-2468.

Tomiki, T., Saito, T., Ueki, M., Konno, H., Asaoka, T., Suzuki, R., Uramoto, M., Kakeya, H., and Osada, H. (2006). RIKEN Natural Products Encyclopedia (RIKEN NPEdia), a chemical database of RIKEN Natural Products Depository (RIKEN NPDepo). J. Comp. Aid. Chem. *7*, 157-162.

Towbin, H., Bair, K.W., DeCaprio, J.A., Eck, M.J., Kim, S., Kinder, F.R., Morollo, A., Mueller, D.R., Schindler, P., Song, H.K., et al. (2003). Proteomics-based target identification: bengamides as a new class of methionine aminopeptidase inhibitors. J. Biol. Chem. *278*, 52964-52971.

Van den Bergh, G., and Arckens, L. (2004). Fluorescent two-dimensional difference gel electrophoresis unveils the potential of gel-based proteomics. Curr. Opin. Biotechnol. *15*, 38-43.

Vlahos, C.J., Matter, W.F., Hui, K.Y., and Brown, R.F. (1994). A specific inhibitor of phosphatidylinositol 3-kinase, 2-(4-morpholinyl)-8-phenyl-4H-1-benzopyran-4-one (LY294002). J. Biol. Chem. *269*, 5241-5248.

Whitesell, L., Mimnaugh, E.G., De Costa, B., Myers, C.E., and Neckers, L.M. (1994). Inhibition of heat shock protein HSP90-pp60v-src heteroprotein complex formation by benzoquinone ansamycins: essential role for stress proteins in oncogenic transformation. Proc. Natl. Acad. Sci. U. S. A. *91*, 8324-8328.

Yaguchi, S., Fukui, Y., Koshimizu, I., Yoshimi, H., Matsuno, T., Gouda, H., Hirono, S., Yamazaki, K., and Yamori, T. (2006). Antitumor activity of ZSTK474, a new phosphatidylinositol 3-kinase inhibitor. J. Natl. Cancer Inst. *98*, 545-556.

Table 1. Expression Data of Identified Spots in HeLa Cells Treated with Geldanamycin or Radicicol.

	Master number of spots and gene name of identified proteins														
	673 *HSP90AB1*	713 *EEF2*	714 *EEF2*	971 *HSPA5*	983 *HSPA5*	998 *HSPA9B*	1114 *HSPA1B*	1127 *HSPA1B*	1295 *HSPD1*	1429 *CAP1*	1484 *FSCN1*	1579 *PDIA6*	2014 *AKR1C2*	2372 *HSPB1*	2382 *HSPB1*
Geldanamycin 0.005 μM	1.02	0.97	0.95	1.03	1.01	0.95	1.05	1.10	1.02	0.96	0.97	1.04	0.95	1.04	0.98
Geldanamycin 0.05 μM	0.97	0.93	0.95	1.07	1.04	1.03	2.74**	3.40**	1.19*	0.96	0.96	1.02	0.91*	1.41*	1.43**
Geldanamycin 0.5 μM	1.29**	0.71**	0.63**	2.26**	1.29*	1.39**	7.22**	8.94**	1.75**	0.61**	0.71**	1.19**	0.66**	2.38**	1.90**
Geldanamycin 5 μM	1.31**	0.66**	0.59**	5.90**	2.70**	1.31**	7.33**	9.20**	1.62**	0.39**	0.72**	1.44**	0.69**	2.48**	1.82**
Geldanamycin 10 μM	1.41**	0.70**	0.55**	5.72**	2.71**	1.41**	8.05**	9.26**	1.64**	0.40**	0.71**	1.42**	0.66**	2.64**	1.75**
Radicicol 10 μM	1.19*	0.82*	0.72**	2.60**	1.28*	1.28*	7.43**	9.39**	1.34**	0.55**	0.75**	1.07	1.06	2.11**	1.65**

The mean ratios of identified spots between control and compound-treated cells are listed. Non-repeated measures ANOVA and Dunnett's test for post hoc analysis were performed. Asterisks indicate significant differences from respective controls (* $P < 0.05$, ** $P < 0.01$).

Table 2. Compounds for Proteomic Analysis by 2D-DIGE

Compounds	Target	IC_{50} (μM)[a]	Conc. (μM)[b]	Ref
Actinomycin D	RNA synthesis	0.0022	0.015	Sobell, 1985
Bafilomycin A1	V-ATPase	0.0035	0.01	Bowman, et al., 1988
Brefeldin A	Protein transport	0.023	0.05	Klausner, et al., 1992
Concanamycin A	V-ATPase	0.002	0.005	Huss, et al., 2002
Cycloheximide	Protein synthesis	0.17	2	Obrig, et al., 1971
Cytochalasin D	Actin	0.32	1	Cooper, 1987
Daunomycin	DNA synthesis	0.034	1	Aubel-Sadron and Londos-Gagliardi, 1984
Etoposide	Topoisomerase II	3	50	Liu, 1989
Geldanamycin	HSP90	0.18	0.5	Whitesell, et al., 1994
ICRF-193	Topoisomerase II	2	50	Roca, et al., 1994
Jasplakinolide	Actin	0.038	0.1	Bubb, et al., 1994
LY294002	PI3 kinase	12	42	Vlahos, et al., 1994
MG-132	Proteasome	0.24	1	Lee, D.H., and Goldberg, A. L. 1998
Nocodazole	Tubulin	0.027	5	Lin and Hamel, 1981
Okadaic acid	Phosphatase	0.014	0.03	Bialojan and Takai, 1988
Radicicol	HSP90	2.1	10	Schulte, et al., 1998
Staurosporine	Protein kinase	0.03	0.3	Rüegg and Burgess, 1989
Tunicamycin	N-linked oligosaccharide synthesis	0.27	5	Takatsuki, et al., 1971
Vinblastine	Tubulin	0.0031	0.01	Rai and Wolff, 1998

[a] The 50% inhibitory concentration of HeLa cell growth.

[b] Concentrations used for proteome analysis

(A)

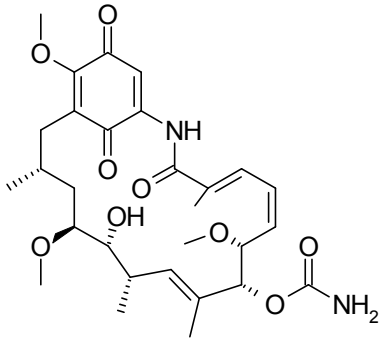

Geldanamycin (**1**)

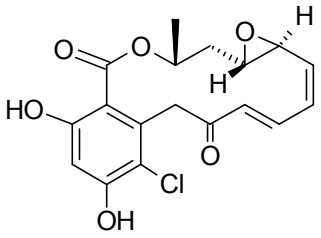

Radicicol **(2)**

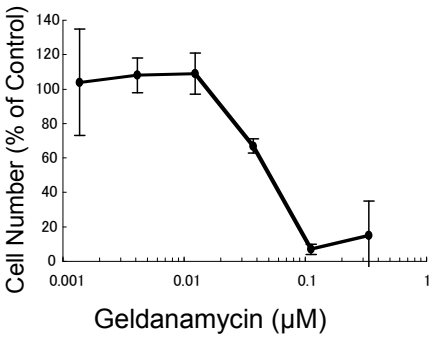

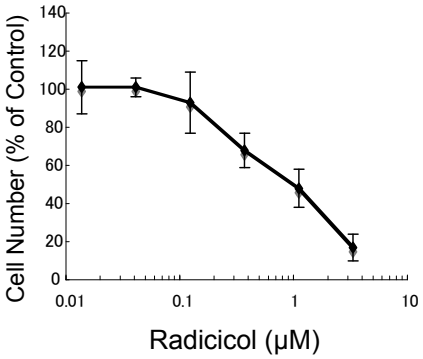

(B)

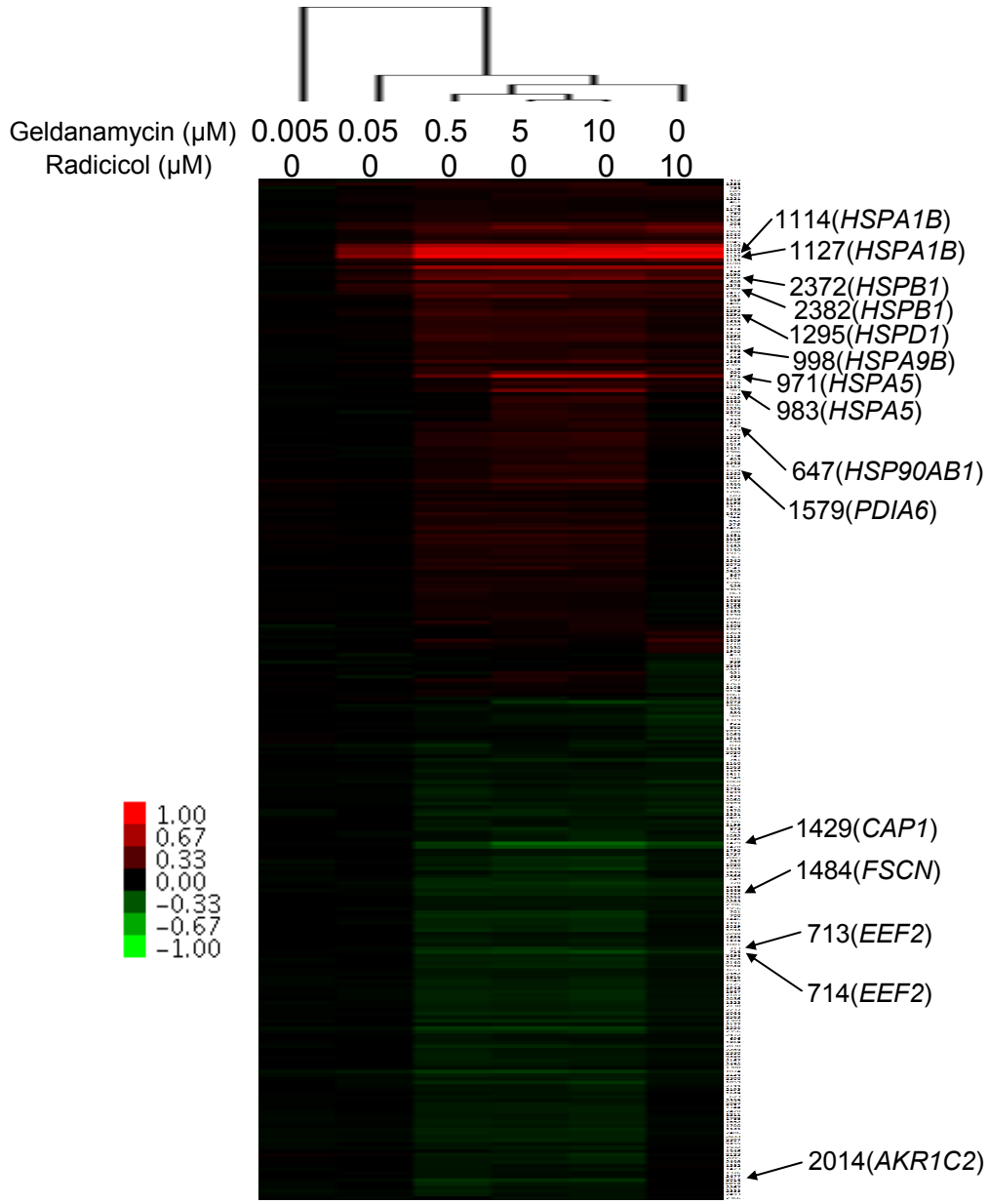
Geldanamycin (μM) 0.005 0.05 0.5 5 10 0
Radicicol (μM) 0 0 0 0 0 10
1114(HSPA1B)
1127(HSPA1B)
2372(HSPB1)
2382(HSPB1)
1295(HSPD1)
998(HSPA9B)
971(HSPA5)
983(HSPA5)
647(HSP90AB1)
1579(PDIA6)
1429(CAP1)
1484(FSCN)
713(EEF2)
714(EEF2)
2014(AKR1C2)
1.00
0.67
0.33
0.00
-0.33
-0.67
-1.00

(C)

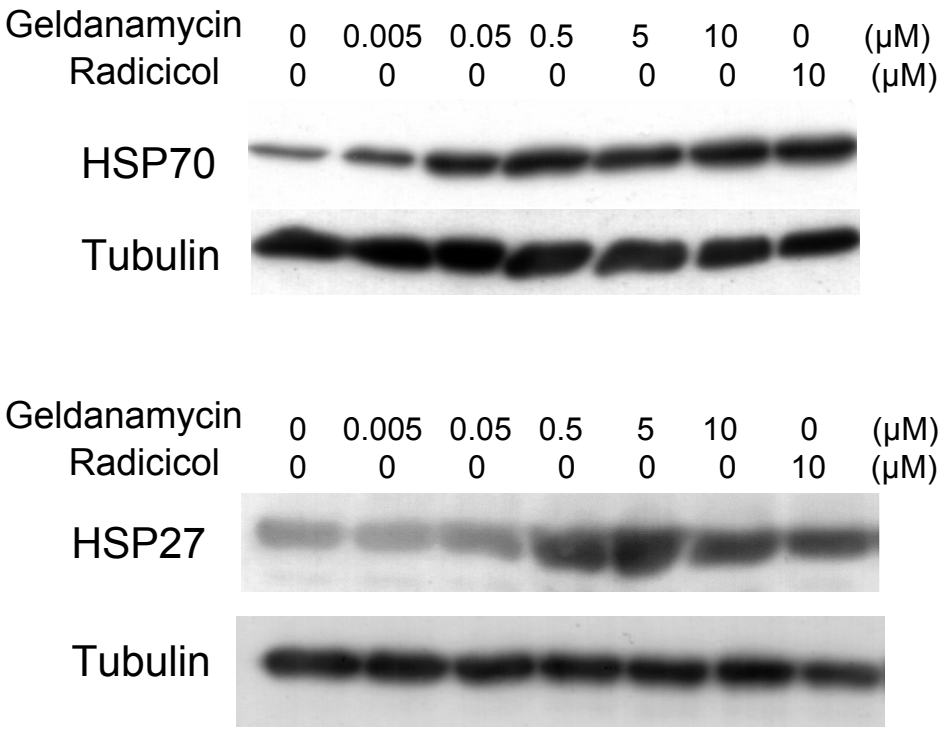
Geldanamycin 0 0.005 0.05 0.5 5 10 0 (μM)
Radicicol 0 0 0 0 0 0 10 (μM)
HSP70
Tubulin
Geldanamycin 0 0.005 0.05 0.5 5 10 0 (μM)
Radicicol 0 0 0 0 0 0 10 (μM)
HSP27
Tubulin

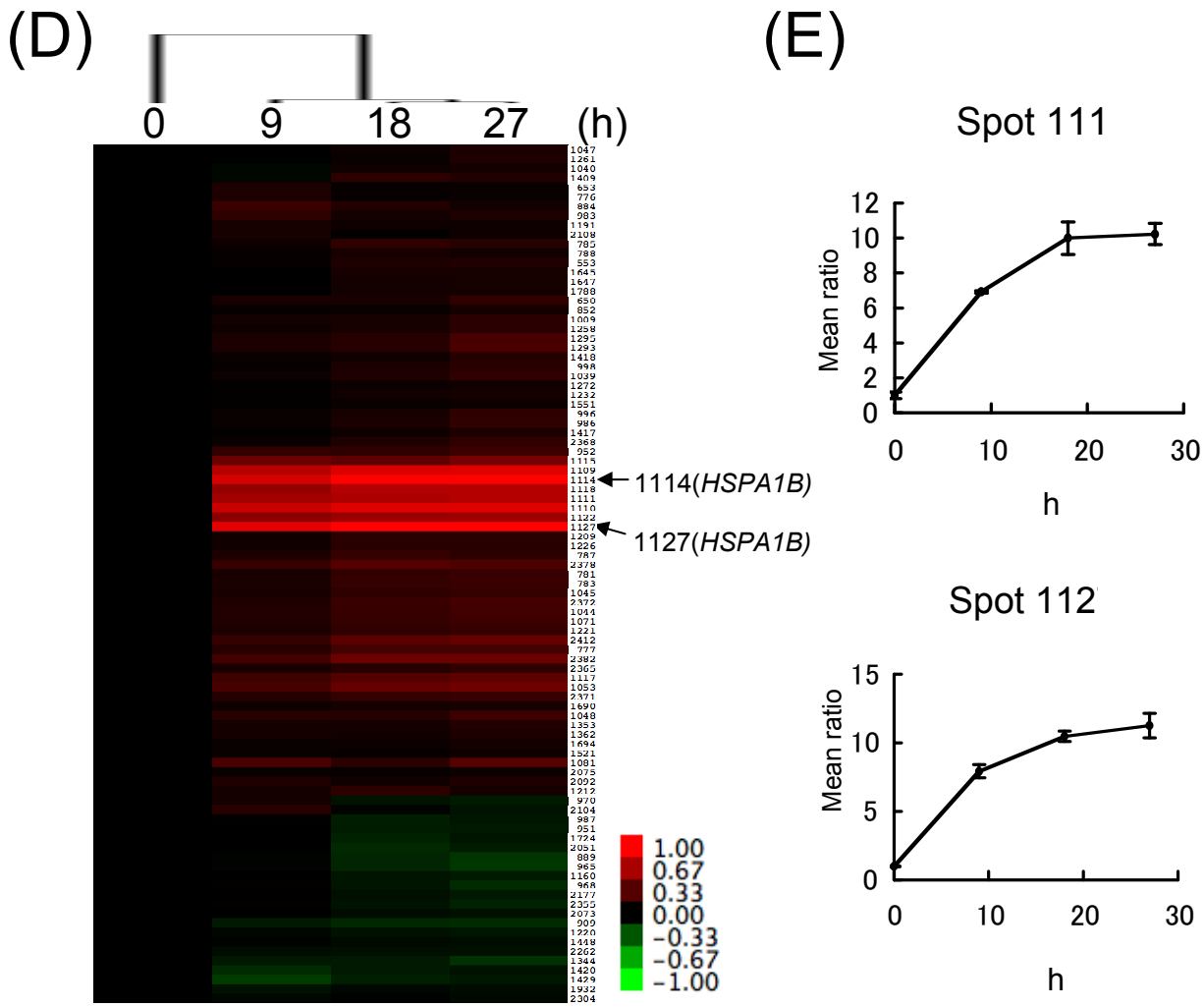
(D)
0
9
18
27
(h)
1114(HSPA1B)
1127(HSPA1B)
1.00
0.67
0.33
0.00
-0.33
-0.67
-1.00
(E)
Spot 111
Mean ratio
h
Spot 112
Mean ratio
h

Figure 2A

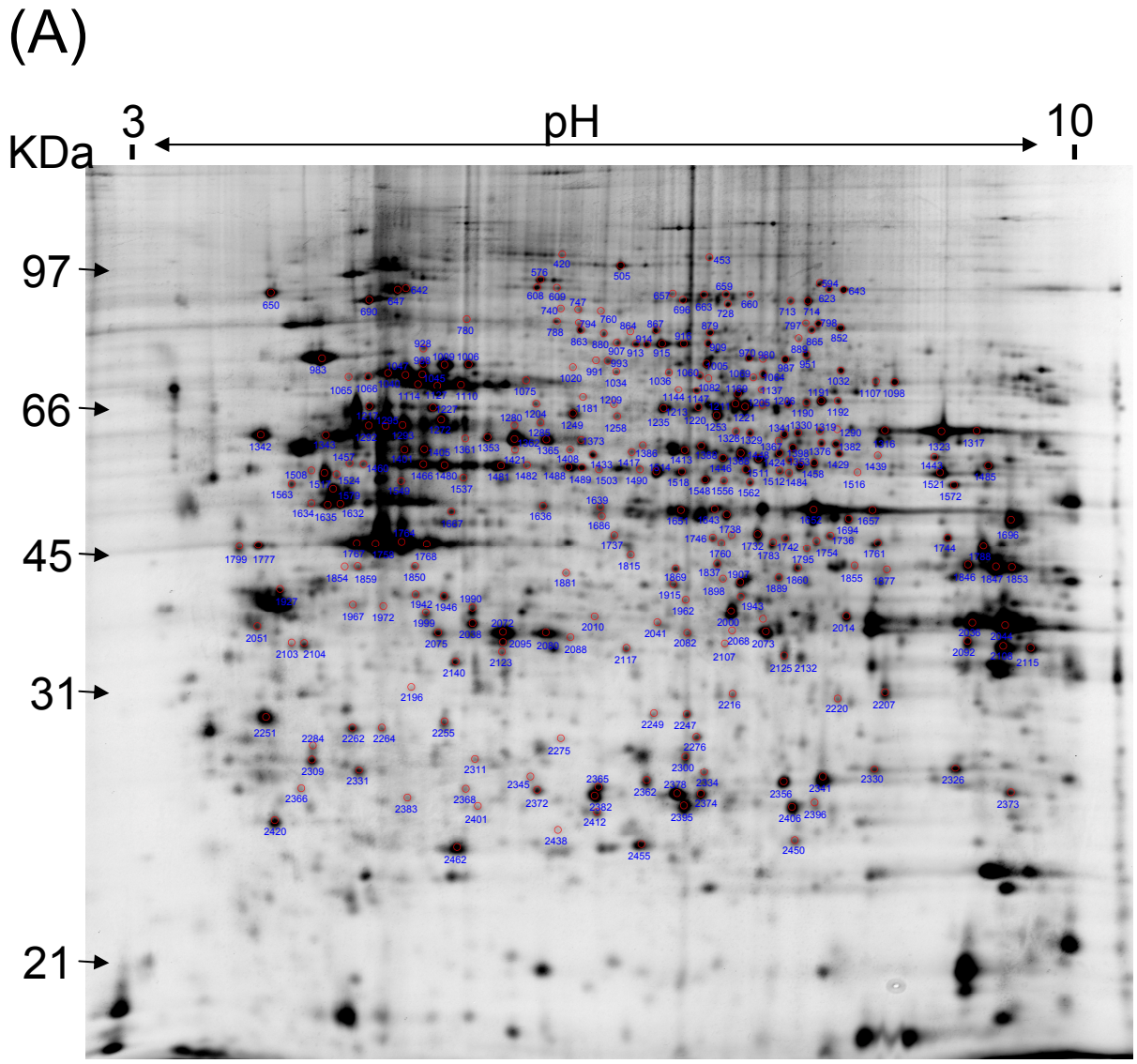

Figure 2B

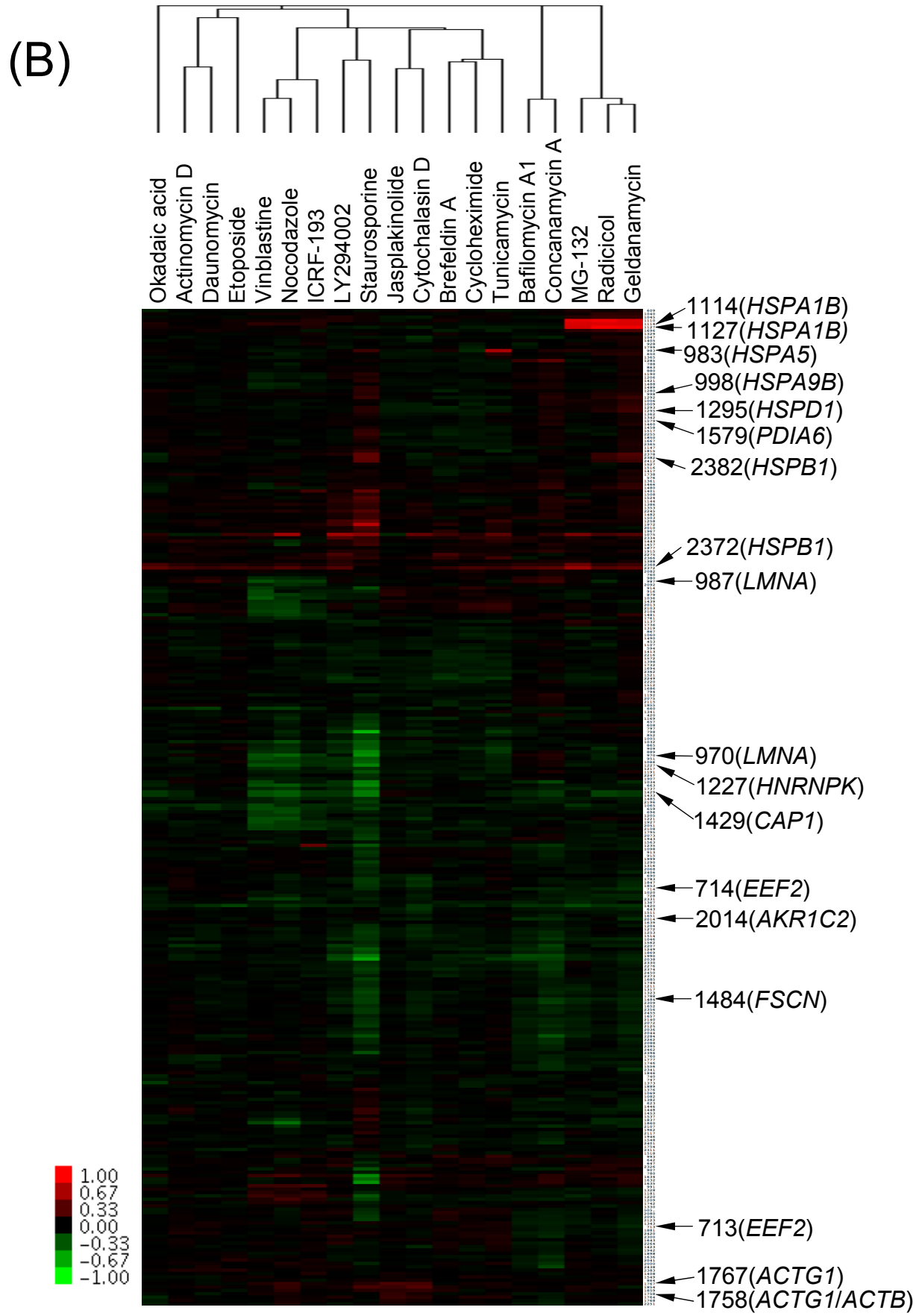
(B)
Okadaic acid
Actinomycin D
Daunomycin
Etoposide
Vinblastine
Nocodazole
ICRF-193
LY294002
Staurosporine
Jasplakinolide
Cytochalasin D
Brefeldin A
Cycloheximide
Tunicamycin
Bafilomycin A1
Concanamycin A
MG-132
Radicicol
Geldanamycin
1114(HSPA1B)
1127(HSPA1B)
983(HSPA5)
998(HSPA9B)
1295(HSPD1)
1579(PDIA6)
2382(HSPB1)
2372(HSPB1)
987(LMNA)
970(LMNA)
1227(HNRNPK)
1429(CAP1)
714(EEF2)
2014(AKR1C2)
1484(FSCN)
713(EEF2)
1767(ACTG1)
1758(ACTG1/ACTB)
1.00
0.67
0.33
0.00
-0.33
-0.67
-1.00

Figure 2C

(C)

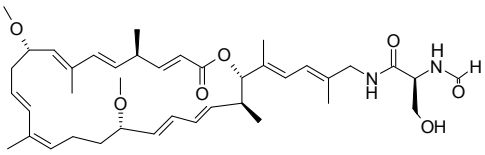

Iejimalide A (**3**)

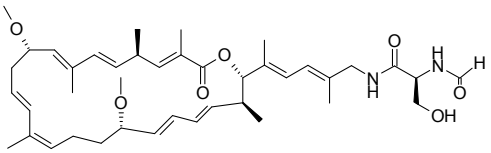

Iejimalide B (**4**)

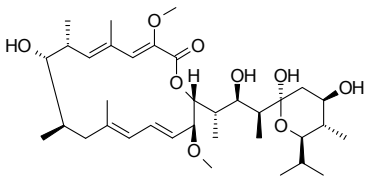

Bafilomycin A1 (**5**)

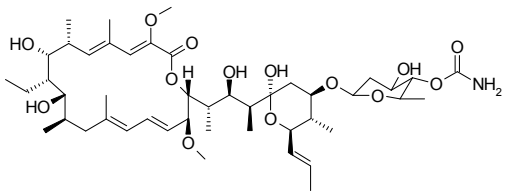

Concanamycin A (**6**)

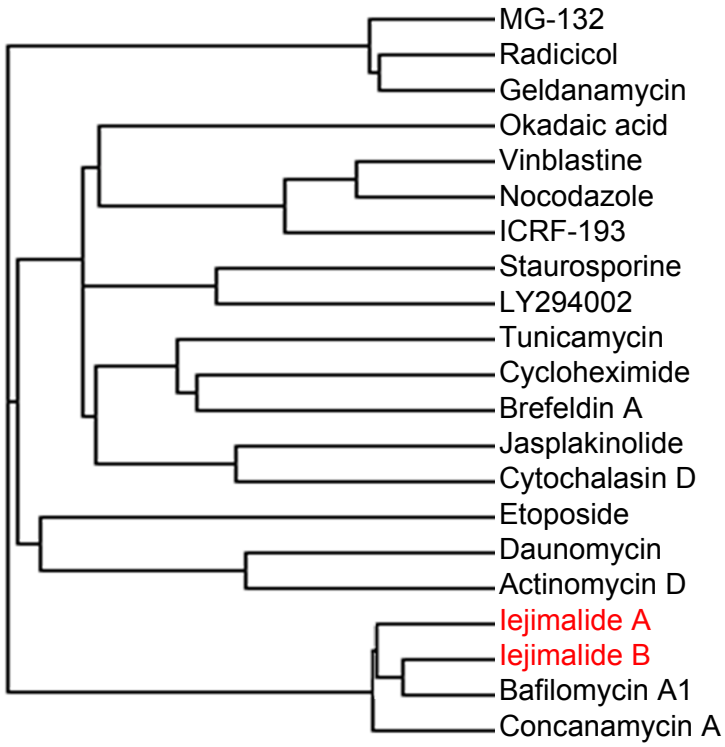

Figure 3

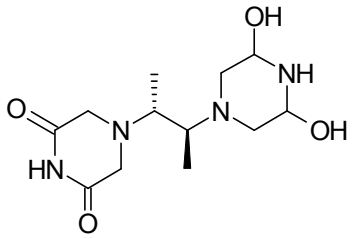

ICRF-193 (**7**)

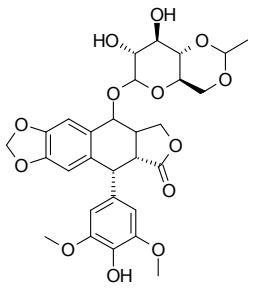

Etoposide (**8**)

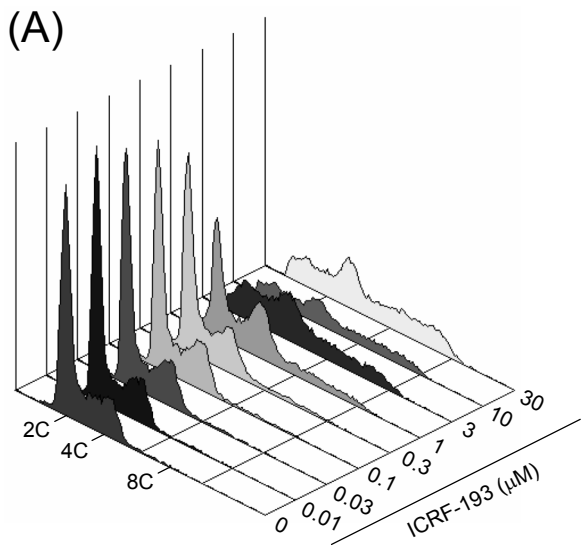

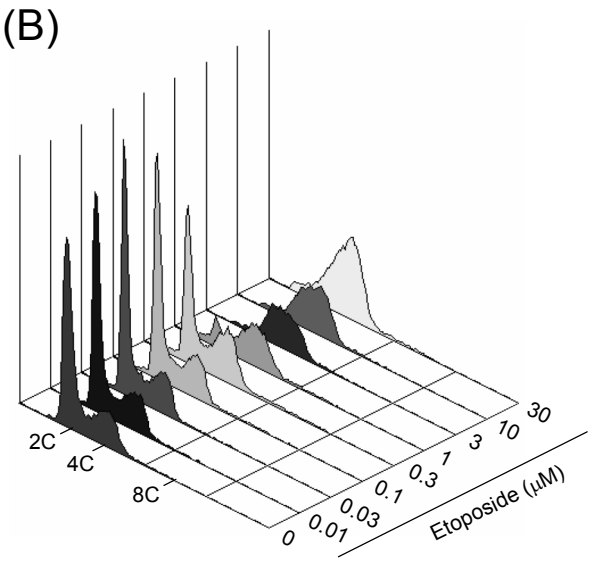

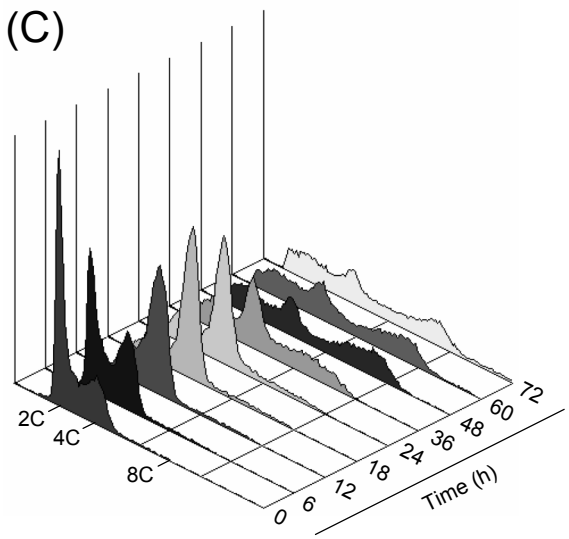

ICRF-193

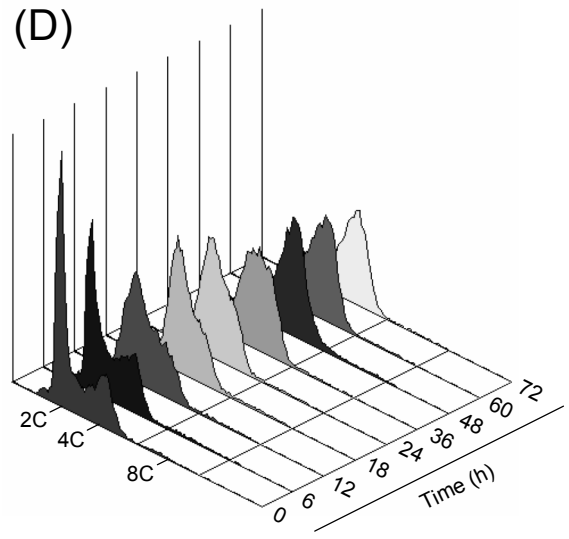

Etoposide